Breakdown of the *k*-conservation rule in quantized Auger recombination in $Si_{1-x}Ge_x$ nanocrystals

Kei Ueda,[1] Takeshi Tayagaki,[1] Masatoshi Fukuda,[2] Minoru Fujii,[2] and Yoshihiko Kanemitsu[1,*]
[1]*Institute for Chemical Research, Kyoto University, Uji, Kyoto 611-0011, Japan*
[2]*Department of Electrical and Electronic Engineering, Kobe University, Kobe 657-8501, Japan*
(Received 9 April 2012; revised manuscript received 22 August 2012; published 22 October 2012)

Dynamics of quantized Auger recombination in $Si_{1-x}Ge_x$ nanocrystals (NCs) embedded in SiO_2 films was studied by femtosecond intraband pump-probe spectroscopy. The temporal change of the electron-hole pair number under strong photoexcitation was well explained by the quantized Auger recombination model that considered the size distribution of NCs. On the basis of the dependence of the Auger decay rate on temperature and Ge composition, we confirmed the occurrence of breakdown of the *k*-conservation rule in quantized Auger recombination in Si and $Si_{1-x}Ge_x$ NCs.

DOI: 10.1103/PhysRevB.86.155316 PACS number(s): 78.67.Hc, 73.21.La, 73.90.+f, 78.47.jb

I. INTRODUCTION

Over the past two decades, the optical properties of semiconductor nanocrystals (NCs) have been studied extensively, because the size dependence of these optical properties opens up avenues for their unique applications in fields such as optoelectronics and biotechnology.[1–6] Semiconductor NCs exhibit fascinating functional properties beyond those of bulk crystals[7,8] and also provide an excellent stage for experimental studies of many-body effects of electron-hole (*e-h*) pairs in optical processes in semiconductors.[9,10] Quantum confinement of *e-h* pairs and reduced dielectric constants in NCs enhance the Coulomb interactions, leading to multiparticle processes such as Auger recombination, i.e., the process by which *e-h* recombination energy is transferred to another electron or hole[9,11,12] and multiple-exciton generation, i.e., the process by which a single photon creates two or more *e-h* pairs.[13–18] In NCs, quantization of Auger recombination rates occurs, and a quantized Auger process causes rapid nonradiative recombination of multiple *e-h* pair states in NCs.[9,11,12] Investigations of unique NC lasers and solar cells have led to intensive research interest in nonradiative recombination in NCs.[19–21] Nonradiative Auger recombination governs both the carrier density and the carrier lifetime and therefore influences the performance of lasers and solar cells. It is known that the Auger decay rate in semiconductor NCs depends strongly on their size, shape, and surface structure.[9,22–28] However, the microscopic mechanism of Auger recombination remains unclear.

In bulk crystals, the *k*-conservation rule plays an essential role in determining the three-carrier Auger decay rate, because the third carrier needs to gain both the energy and momentum of the recombined *e-h* pair. Owing to the *k*-conservation rule, the Auger decay rate in bulk crystals is very sensitive to temperature; no-phonon Auger decay rate depends exponentially on the temperature, or phonon-assisted Auger decay rate is determined by thermal distribution of phonons.[29] For study on the effect of the *k*-conservation rule on carrier recombination processes, crystalline Si is an excellent material, because bulk crystal Si is an indirect band-gap semiconductor. Phonon-assisted processes dominate radiative recombination, where momentum-conserving phonons are transversal-optical and transversal-acoustic phonons in bulk crystals.[30–32] The Auger lifetimes in bulk Si depend on temperature, because of the *k*-conservation rule.[33–36] Phonon-assisted and no-phonon Auger recombination processes have been discussed.[33,34,36]

In NCs, the breakdown or relaxation of the *k*-conservation rule in recombination processes has been intensively discussed. It has been well known that in Si NCs, the dominant radiative recombination is the momentum-conserving-phonon-assisted transitions, similar to the case of Si bulk crystals, although no-phonon transition intensity increases in small NCs.[37–40] On the other hand, the impact of the *k*-conservation rule on the quantized Auger recombination rate in NCs remains unclear.[23,41] Very few studies have investigated the relaxation of translational-momentum conservation due to the quantum confinement, which manifests in phenomena such as temperature dependence of the Auger decay rate,[28] because the *k*-conservation rule causes temperature-dependent Auger rate in bulk crystals. However, almost all previous experimental studies have been conducted using NC solutions, and then the Auger rate has not been studied over a wide temperature range. To study the temperature dependence of the Auger rate, solid NC samples have an advantage over NC solution samples. Therefore, a systematic study of the Auger recombination mechanism in *solid NC films* is essential for understanding the physics of multiple *e-h*-pair states in NCs and device applications of NCs.

In this work, we report on the Auger recombination in Si and $Si_{1-x}Ge_x$ NCs embedded in SiO_2 matrices as studied by femtosecond intraband pump-probe spectroscopy with varying temperature. The embedded solid structure enabled us to study the temperature dependence of the carrier recombination processes. The temperature dependence of the Auger decay rate is clearly indicative of the breakdown of the *k*-conservation in Auger recombination in $Si_{1-x}Ge_x$ NCs. Temporal changes of the *e-h*-pair number under strong photoexcitation are well explained by a quantized Auger recombination model that considers the size distribution of NCs.

II. EXPERIMENT

$Si_{1-x}Ge_x$ nanocrystals were prepared by a cosputtering method. Details of the preparation procedure and structural characterization can be found elsewhere.[42,43] Si, Ge, and SiO_2 sputtering targets were simultaneously sputtered in Ar gas at 0.3 Pa using a multitarget sputtering apparatus. After

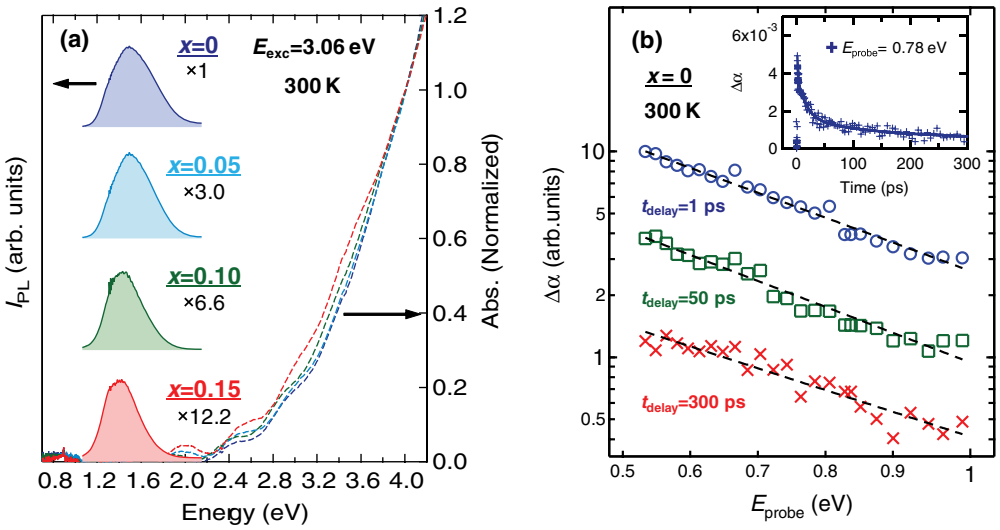

FIG. 1. (Color online) (a) PL and optical absorption spectra of $Si_{1-x}Ge_x$ NC samples. (b) TA signals as a function of probe pulse energy at different delay times. The broken curves show the fitting results obtained using a $1/E^2$ dependence. The inset shows a typical decay profile of the TA signal.

sputtering, the films were annealed in N_2 gas ambient at 1100 °C to grow $Si_{1-x}Ge_x$ NCs in SiO_2 matrices. The thickness of the films was about 500 nm. The average NC diameter of about 4 nm and the size distribution of NCs were estimated from transmission electron microscopy images, and the sizes of $Si_{1-x}Ge_x$ NCs were almost the same as Si NCs.[42,43]

The 150-fs laser pulses from a Ti:sapphire regenerative amplifier system operating at 1 kHz were used in the pump-probe experiment. A pump pulse with a photon energy of 2.34 eV and a probe pulse with a photon energy of 0.55–0.98 eV, both derived from the optical parametric amplifier system, were employed. The laser spot size on the sample surface was measured carefully by the knife-edge method. Time-integrated photoluminescence (PL) spectra were measured using a liquid-nitrogen-cooled InGaAs array detector and a Si charge-coupled device. The PL lifetime was measured using a gated-photon counting system equipped with a photomultiplier. All measurements were performed over a wide temperature range (from 8 to 400 K) in a cryostat.

III. RESULTS AND DISCUSSION

Figure 1(a) shows the absorption and PL spectra of the $Si_{1-x}Ge_x$ NCs. The PL energy in Si NCs ($x = 0$) is around 1.46 eV, which is consistent with the band-gap energy reported in previous theoretical and experimental studies of Si NCs with a diameter of about 4 nm.[32,42] With an increase in Ge composition, both the PL peak and the absorption edge energies shift slightly to the low-energy side and the PL intensity decreases. We confirmed that the PL decay in the microsecond time region is consistent with previously reported data.[42]

To study carrier recombination dynamics, we employed femtosecond transient absorption (TA) spectroscopy. On account of the indirect band gap of the $Si_{1-x}Ge_x$ NCs, we probed the carrier recombination dynamics on the basis of photoinduced intraband absorption changes.[12,14,44] The inset of Fig. 1(b) shows typical TA decays monitored at the probe energy of 0.78 eV. The magnitude of the TA signal was dependent on the probe energy. This dependence at different delay times is summarized in Fig. 1(b), where the excitation intensity is about 1300 $\mu J/cm^2$. The TA signals are well described by a free carrier model with a $1/E^2$ dependence over the range of 0.55 to 0.98 eV [shown by the broken curves in Fig. 1(b)]. Therefore, the TA signals probed at low photon energies, i.e., below the PL energy (~1.5 eV), originate from photogenerated free-carrier absorption. We set the photon energy of the probe pulse, E_{probe}, at 0.83 eV.

Figure 2 shows the dynamics of the TA signal for Si NCs ($x = 0$) as a function of the excitation intensity. The photon energy of the pump pulse was set at 2.34 eV, in which the optical absorption is so weak that all the NCs are illuminated homogeneously at the same excitation intensity. The signal intensities were normalized at the delay time of 1000 ps, because irrespective of the excitation intensity, the decay

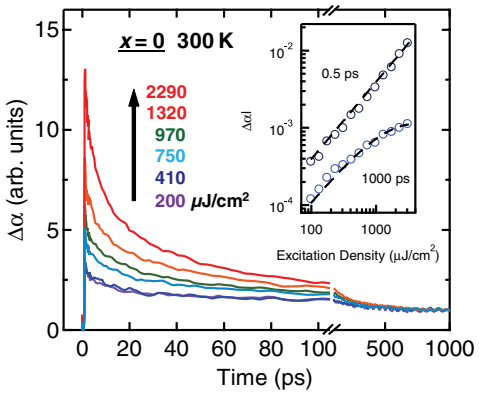

FIG. 2. (Color online) Temporal changes of the TA signal ($\Delta\alpha$) at 0.83 eV under 2.34 eV excitation, with excitation intensities of 200, 410, 750, 970, 1320, and 2290 $\mu J/cm^2$. The inset shows the TA signals at delay times at 0.5 and 1000 ps as a function of the excitation intensity. The broken curves show the fitting results.

curves at a large decay time are very similar to each other and are determined by the recombination of a single e-h pair. Under high-intensity excitation, a fast decay component appears after photoexcitation. The appearance of this component indicates the Auger recombination of multiple e-h pairs. The inset of Fig. 2 shows TA signals at delay times of 0.5 and 1000 ps as a function of the excitation intensity. The TA signal at 0.5 ps increases with increasing excitation intensity. After the Auger recombination is complete, the signal intensity at the 1000-ps delay time follows the relation[11]

$$\Delta\alpha \propto 1 - \exp(-\sigma_{\rm abs} j_{\rm p}), \tag{1}$$

where $\sigma_{\rm abs}$ and $j_{\rm p}$ are the absorption cross section and the photon flux, respectively. Here we assumed a Poisson distribution of the initial number of e-h-pairs, N, in a given NC:

$$P_N(t_{\rm delay} = 0\,{\rm ps}) = \frac{e^{-\langle N\rangle}\langle N\rangle^N}{N!}. \tag{2}$$

By fitting the signal intensity at 1000 ps (e.g., broken curve in the inset of Fig. 2), we extracted the mean $\sigma_{\rm abs}$ value of 2.7×10^{-16} and 4.1×10^{-16} cm^{-2} for the Si NC ($x = 0$) and the $Si_{1-x}Ge_x$ NC ($x = 0.15$) samples, respectively. The average number of e-h pairs in NCs, $\langle N\rangle$, determined using the obtained $\sigma_{\rm abs}$, was used in subsequent discussions.

Figure 3 shows the differential decay profiles, obtained by the subtraction of the slow decay component at $\langle N\rangle \sim 0.2$ from the decay profiles under the high-excitation condition of $\langle N\rangle \geqslant 0.9$. The slow component was independent of the excitation intensity, but exhibited the nonexponential decay, which was caused from the inhomogeneous size distribution and was also observed in the PL decay measurements. The differential decay profiles are indicative of multicarrier decay. In the quantized Auger recombination model, the probability distribution of the N e-h pairs existing in one NC, $P_N(t)$, obeys the following relation:[11,12,45]

$$\frac{d}{dt}P_N(t) = -\frac{1}{\tau_N}P_N(t) + \frac{1}{\tau_{N+1}}P_{N+1}(t), \tag{3}$$

$$\tau_N^{-1} = \frac{N^2(N-1)}{2}\gamma_{\rm Auger}, \tag{4}$$

where $\gamma_{\rm Auger}$ is a constant. However, a simple quantized Auger recombination model could not explain the obtained decay profiles. Then, we included the size distribution of NCs in the model. In fact, the size distribution of the $Si_{1-x}G_x$ NCs prepared by the sputtering in this study was broad. We considered an average diameter of 4.0 nm and a dispersion of 20% for the size distribution of NCs described by Gaussian functions.[43] Here we assumed that the absorption cross section is proportional to the square of the NC diameter, D, i.e., $\sigma_{\rm abs}(D) \propto D^2$, and obtained the initial condition of the population probability. The size dependence of the Auger decay rate, $\gamma_{\rm Auger}(D) \propto D^{-3}$, was also assumed in the analysis.[23,27] The fitting results are indicated by the broken curves in Fig. 3. Over wide delay times (>10 ps), the calculated curves well reproduce the experimental results. Thus, we can determine the Auger decay rates of the samples from the calculated curves. We conclude that the recombination dynamics of multiple e-h-pair states are well explained by the quantized Auger recombination model that considers the size distribution of NCs.

Figure 4 shows the differential decay profile under strong photoexcitation, $\langle N\rangle \sim 3$, for the NC samples with different Ge compositions ($x = 0.05, 0.10, 0.15$). At high Ge compositions, a fast decay component, with a decay time of a few picoseconds, appeared even under the weak excitation condition. The intensities of the differential signals were normalized at the delay time of 0 ps. The decay time reduced with increasing Ge composition, x. The decay times were obtained by using the above-mentioned quantized Auger recombination model, as discussed in Fig. 3. We obtained the Auger decay time of two e-h pairs, $\tau_2 = 80$ ps for $x = 0$, which is fairly consistent with $\tau_2 \sim 40$ ps in Ref. 14 ($D \sim 3.8$ nm) and $\tau_2 \sim 100$ ps reported in Ref. 46 ($D \sim 3$ nm). The inset of Fig. 4 shows the Auger decay time τ_2 as a function of the Ge composition. The Auger decay time decreases with increasing Ge composition. Even though the no-phonon Auger recombination rate in bulk semiconductors depends exponentially on the inverse of the band-gap energy,[29] the reduction in the band-gap energy is too small to explain the enhanced Auger decay rates in the

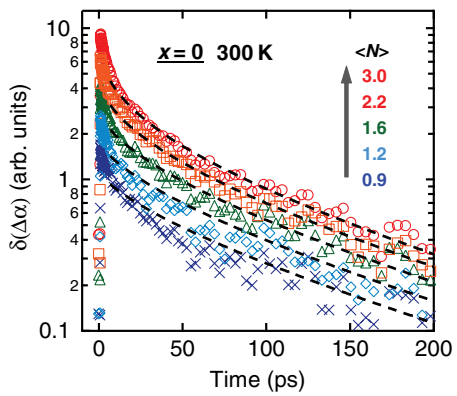

FIG. 3. (Color online) Fitting results of differential TA signals $\delta(\Delta\alpha)$ using the quantized Auger recombination model including the size distribution.

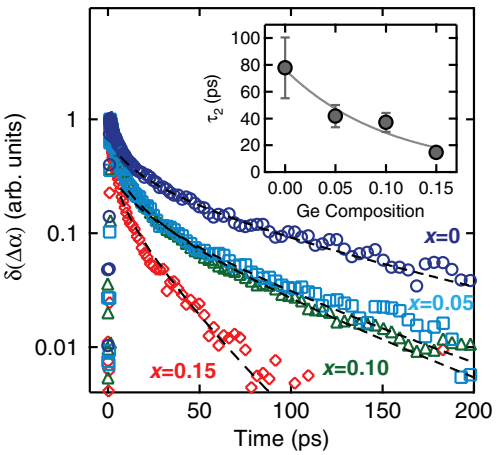

FIG. 4. (Color online) Differential TA $\delta(\Delta\alpha)$ dynamics under strong photoexcitation $\langle N\rangle \sim 3$ with various Ge compositions: x ($x = 0, 0.05, 0.10, 0.15$). The broken curves show the fitting results obtained using the quantized Auger recombination model including the size distribution. Inset: Auger decay time τ_2^{-1} as a function of the Ge composition x.

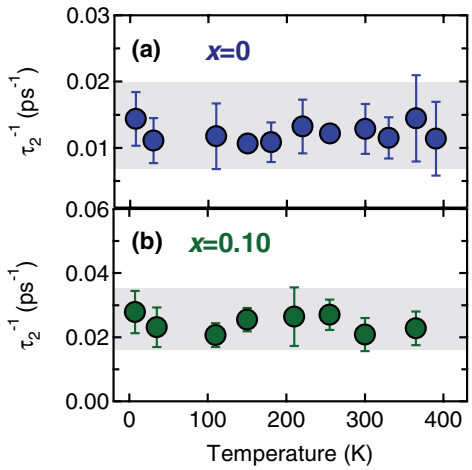

FIG. 5. (Color online) Temperature dependence of the Auger decay rate $\tau_2{}^{-1}$. (a) $x = 0$ and (b) $x = 0.10$.

$Si_{1-x}Ge_x$ NCs [see Fig. 1(a)]. In contrast, the surface defects in $Si_{1-x}Ge_x$ NCs increase with increasing Ge composition,[47] which is consistent with the reduced PL decay time.[48] Thus, at present, we consider that enhanced Auger recombination in NCs with a high Ge composition is partially related to the scattering process assisted by alloy disorder and a high NC surface-state density; alloy disorder in mix crystals and surface scattering enhance the Auger rate in $Si_{1-x}Ge_x$ NCs with high Ge compositions.

Figure 5 shows the temperature dependence of the Auger decay rate, $\tau_2{}^{-1}$, in NCs with $x = 0$ and 0.10. In both samples, the Auger decay rates remain almost constant over the temperature range of 8–400 K. In bulk semiconductors, the Auger decay rate is restricted by strict conservation requirements of energy and momentum, because the third electrons need to gain both the energy and momentum of the recombined *e-h* pairs. Therefore, the no-phonon Auger recombination rate depends exponentially on the temperature, $\tau_2^{-1} \propto \exp(-E_a/k_BT)$, where E_a is the activation energy.[29] In contrast, in a phonon-assisted Auger recombination model, the Auger decay rate is determined by the phonon distribution and follows the relation[33,49]

$$\tau_2^{-1} \propto \frac{\exp(E_{\text{phonon}}/k_BT) + 1}{\exp(E_{\text{phonon}}/k_BT) - 1}, \tag{5}$$

where E_{phonon} is the phonon energy. In bulk Si crystal, the experimentally observed Auger decay rate depends on the temperature.[33,34] Such a weak temperature dependence of the Auger rate can be explained by the phonon-assisted Auger recombination model, rather than the no-phonon Auger recombination model.[33–35] Even though the detailed mechanism of Auger recombination has been still debated,[36] the Auger decay rate in bulk Si crystals depends on the temperature, owing to the *k*-conservation rule in recombination processes. In contrast, in the NCs in our study, the Auger recombination rate is almost independent of temperature over the wide temperature range. This clearly shows that the *k*-conservation rule in Auger recombination breaks down in Si NCs.

Finally, we discuss the impact of phonon-assisted momentum conservation on radiative and Auger recombination processes in NCs. No temperature dependence of the Auger decay rate is observed in $Si_{1-x}Ge_x$ NCs, as shown in Fig. 5(b). Further, the PL spectra of $Si_{1-x}Ge_x$ NCs show the unclear phonon structures owing to alloy disorder and lattice disorder: A previous PL study has suggested the breakdown of the *k*-conservation rule in $Si_{1-x}Ge_x$ NCs.[48] Thus, temperature-independent Auger recombination is consistent with the broken translational symmetry in $Si_{1-x}Ge_x$ NCs. Alloy disorder and surface scattering enable Auger transitions for a broad range of final states,[25] and cause the enhancement of the Auger rate in $Si_{1-x}Ge_x$ NCs with high Ge compositions.

In contrast, in previous PL studies of Si NCs, phonon-assisted radiative transition was dominant despite the observation of a no-phonon transition.[37–40] In indirect band-gap semiconductors, phonon assistance is necessary to conserve the momentum in the radiative recombination between electrons and holes. Even in small NCs, phonon assistance with large momentum or further large uncertainty of momentum is necessary. However, our findings show that the phonon assistance is not necessary for Auger recombination in Si NCs. This difference is explained by the fact that while PL is related to *two*-carrier recombination, Auger recombination is based on *three*-carrier collisions. In Auger recombination, the recombination energy of *e-h* pairs is transferred to another electron or hole, where the momentum of the geminate *e-h* pair is not required to be zero. Thus, Auger recombination will be enhanced if the uncertainty of the momentum increases with decreasing NC size. This explanation is consistent with increased Auger decay rates in $Si_{1-x}Ge_x$ NCs, in which the uncertainty of the momentum is more enhanced owing to alloy disorder. The temperature dependence of the Auger decay rate clearly indicates the breakdown of the *k*-conservation rule in Auger recombination in Si and $Si_{1-x}Ge_x$ NCs.

IV. CONCLUSION

In conclusion, we studied the photocarrier recombination dynamics of Si and $Si_{1-x}Ge_x$ NCs embedded in SiO_2 matrices as a function of the photoexcited *e-h*-pair number and temperature. We found temporal changes of *e-h*-pair number under strong photoexcitation to be well explained by the quantized Auger recombination model that considers the size distribution of NCs. Breakdown of the *k*-conservation rule in Auger recombination was found to occur in indirect-band-gap Si and $Si_{1-x}Ge_x$ NCs.

ACKNOWLEDGMENTS

This study was partly supported by KAKENHI (Grant No. 20104006 to T.T. and Y.K.) from MEXT, KAKENHI (Grant No. 23310077 to M. Fujii) from JSPS, and JST-CREST (to Y.K.).

*kanemitu@scl.kyoto-u.ac.jp

[1] L. Brus, J. Chem. Phys. **90**, 2555 (1986).
[2] Y. Kanemitsu, Phys. Rep. **263**, 1 (1995).
[3] A. P. Alivisatos, J. Phys. Chem. **100**, 13226 (1996).
[4] S. A. Empedocles, R. Neuhauser, K. Shimizu, and M. G. Bawendi, Adv. Mater. **11**, 1243 (1999).
[5] V. I. Klimov, J. Phys. Chem. **110**, 16827 (2006).
[6] A. J. Nozik, Chem. Phys. Lett. **457**, 3 (2008).
[7] C. R. Kagan, C. B. Murray, M. Nirmal, and M. G. Bawendi, Phys. Rev. Lett. **76**, 1517 (1996).
[8] K. Hosoki, T. Tayagaki, S. Yamamoto, K. Matsuda, and Y. Kanemitsu, Phys. Rev. Lett. **100**, 207404 (2008).
[9] V. I. Klimov, A. A. Mikhailovsky, D. W. McBranch, C. A. Leatherdale, and M. G. Bawendi, Science **287**, 1011 (2000).
[10] Y. Kanemitsu, T. J. Inagaki, M. Ando, K. Matsuda, T. Saiki, and C. W. White, Appl. Phys. Lett. **81**, 141 (2002).
[11] V. I. Klimov, J. A. McGuire, R. D. Schaller, and V. I. Rupasov, Phys. Rev. B **77**, 195324 (2008).
[12] A. Ueda, T. Tayagaki, and Y. Kanemitsu, J. Phys. Soc. Jpn. **78**, 083706 (2009).
[13] R. D. Schaller and V. I. Klimov, Phys. Rev. Lett. **92**, 186601 (2004).
[14] M. C. Beard, K. P. Knutsen, P. Yu, J. M. Luther, Q. Song, W. K. Metzger, R. J. Ellingson, and A. J. Nozik, Nano Lett. **7**, 2506 (2007).
[15] G. Nair and M. G. Bawendi, Phys. Rev. B **76**, 081304(R) (2007).
[16] R. Ellingson, M. C. Beard, J. C. Johnson, P. Yu, O. I. Micic, A. J. Nozik, A. Shabaev, and A. L. Efros, Nano Lett. **5**, 865 (2005).
[17] A. Ueda, K. Matsuda, T. Tayagaki, and Y. Kanemitsu, Appl. Phys. Lett. **92**, 233105 (2008).
[18] J. J. H. Pijpers, R. Ulbricht, K. J. Tielrooij, A. Osherov, Y. Golan, C. Delerue, G. Allan, and M. Bonn, Nat. Phys. **5**, 811 (2009).
[19] V. I. Klimov, S. A. Ivanov, J. Nanda, M. Achermann, I. Bezel, J. A. McGuire, and A. Piryatinski, Nature (London) **447**, 441 (2007).
[20] V. Sukhovatkin, S. Hinds, L. Brzozowski, and E. H. Sargent, Science **324**, 1542 (2009).
[21] O. E. Semonin, J. M. Luther, S. Choi, H. Chen, J. Gao, A. J. Nozik, and M. C. Beard, Science **334**, 1530 (2011).
[22] D. I. Chepic, Al. L. Efros, A. I. Ekimov, M. G. Ivanov, V. A. Kharchenko, I. A. Kudriavtsev, and T. V. Yazeva, J. Lumin. **47**, 113 (1990).
[23] I. Robel, R. Gresback, U. Kortshagen, R. D. Schaller, and V. I. Klimov, Phys. Rev. Lett. **102**, 177404 (2009).
[24] H. Htoon, J. A. Hollingsworth, R. Dickerson, and V. I. Klimov, Phys. Rev. Lett. **91**, 227401 (2003).
[25] X. Wang, X. Ren, K. Kahen, M. A. Hahn, M. Rajeswaran, S. Maccagnano-Zacher, J. Silcox, G. E. Cragg, Al. L. Efros, and T. D. Krauss, Nature (London) **459**, 686 (2009); E. Cragg and Al. L. Efros, Nano Lett. **10**, 313 (2010).
[26] S. Taguchi, M. Saruyama, T. Teranishi, and Y. Kanemitsu, Phys. Rev. B **83**, 155324 (2011).
[27] Y. Kobayashi, T. Nishimura, H. Yamaguchi, and N. Tamai, J. Phys. Chem. Lett. **2**, 1051 (2011).
[28] Y. Kobayashi and N. Tamai, J. Phys. Chem. C **114**, 17550 (2010).
[29] P. T. Landsberg, *Recombination in Semiconductors* (Cambridge University Press, Cambridge, 1991).
[30] G. G. Macfarlane, T. P. McLean, J. E. Quarrington, and V. Roberts, Phys. Rev. **111**, 1245 (1958).
[31] P. J. Dean, J. R. Haynes, and W. F. Flood, Phys. Rev. **161**, 711 (1967).
[32] As a review, Y. Kanemitsu, in *Comprehensive Semiconductor Science and Technology*, edited by P. Bhattacharya, R. Fornari, and H. Kamimura, Vol. 2 (Elsevier, Amsterdam, 2011), pp. 196–212.
[33] A. Haug, J. Phys. Chem. Solids **49**, 599 (1988).
[34] K. G. Svantesson and N. G. Nilsson, J. Phys. C **12**, 5111 (1979).
[35] A. R. Guichard, R. D. Kekatpure, M. L. Brongersma, and T. I. Kamins, Phys. Rev. B **78**, 235422 (2008).
[36] D. B. Laks, G. F. Neumark, and S. T. Pantelides, Phys. Rev. B **42**, 5176 (1990).
[37] P. D. J. Calcott, K. J. Nash, L. T. Canham, M. J. Kane, and D. Brumhead, J. Phys.: Condens. Matter **5**, L91 (1993).
[38] M. S. Hybertsen, Phys. Rev. Lett. **72**, 1514 (1994).
[39] Y. Kanemitsu, S. Okamoto, M. Otobe, and S. Oda, Phys. Rev. B **55**, R7375 (1997).
[40] D. Kovalev, H. Heckler, M. Ben-Chorin, G. Polisski, M. Schwartzkopff, and F. Koch, Phys. Rev. Lett. **81**, 2803 (1998).
[41] J. M. Pietryga, K. K. Zhuravlev, M. Whitehead, V. I. Klimov, and R. D. Schaller, Phys. Rev. Lett. **101**, 217401 (2008).
[42] S. Takeoka, K. Toshikiyo, M. Fujii, S. Hayashi, and K. Yamamoto, Phys. Rev. B **61**, 15988 (2000).
[43] S. Takeoka, M. Fujii, and S. Hayashi, Phys. Rev. B **62**, 16820 (2000).
[44] As an example, P. Y. Yu and M. Cardona, *Fundamentals of Semiconductors: Physics and Materials Properties*, 4th ed. (Springer, Berlin, 2010).
[45] V. Barzykin and M. Tachiya, J. Phys.: Condens. Matter **19**, 065105 (2007).
[46] F. Trojanek, K. Neudert, M. Bittner, and P. Maly, Phys. Rev. B **72**, 075365 (2005).
[47] K. Toshikiyo, M. Tokunaga, S. Takeoka, M. Fujii, and S. Hayashi, J. Appl. Phys. **89**, 4917 (2001).
[48] M. Fujii, D. Kovalev, J. Diener, F. Koch, S. Takeoka, and S. Hayashi, J. Appl. Phys. **88**, 5772 (2000).
[49] Y. Yamada, H. Yasuda, T. Tayagaki, and Y. Kanemitsu, Phys. Rev. Lett. **102**, 247401 (2009).